Sensitive bi-enzymatic biosensor based on polyphenoloxidases-gold nanoparticles-chitosan hybrid film-graphene doped carbon paste electrode for carbamates detection

Thiago M.B.F. Oliveira, M. Fátima Barroso, Simone Morais, Mariana Araújo, Cristina Freire, Pedro de Lima-Neto, Adriana N. Correia, Maria B.P.P. Oliveira, Cristina Delerue-Matos

ABSTRACT

A bi-enzymatic biosensor (LACC-TYR-AuNPs-CS/GPE) for carbamates was prepared in a single step by electro- deposition of a hybrid film onto a graphene doped carbon paste electrode (GPE). Graphene and the gold nanopar- ticles (AuNPs) were morphologically characterized by transmission electron microscopy, X-ray photoelectron spectroscopy, dynamic light scattering and laser Doppler velocimetry. The electrodeposited hybrid film was composed of laccase (LACC), tyrosinase (TYR) and AuNPs entrapped in a chitosan (CS) polymeric matrix. Exper- imental parameters, namely graphene redox state, AuNPs:CS ratio, enzymes concentration, pH and inhibition time were evaluated. LACC-TYR-AuNPs-CS/GPE exhibited an improved Michaelis-Menten kinetic constant (26.9 ± 0.5 M) when compared with LACC-AuNPs-CS/GPE (37.8 ± 0.2 M) and TYR-AuNPs-CS/GPE (52.3 ± 0.4 M). Using 4-aminophenol as substrate at pH 5.5, the device presented wide linear ranges, low detection limits ($1.68 \times 10^{-9} \pm 1.18 \times 10^{-10}$-$2.15 \times 10^{-7} \pm 3.41 \times 10^{-9}$ M), high accuracy, sensitivity ($1.13 \times 10^{6} \pm 8.11 \times 10^{4}$-$2.19 \times 10^{8} \pm 2.51 \times 10^{7}$ %inhibition M^{-1}), repeatability (1.2-5.8% RSD), reproducibility (3.2-6.5% RSD) and stability (ca. twenty days) to determine carbaryl, formetanate hydrochloride, propoxur and ziram in citrus fruits based on their inhibitory capacity on the polyphenoloxidases activity. Recoveries at two fortified levels ranged from $93.8 \pm 0.3\%$ (lemon) to $97.8 \pm 0.3\%$ (orange). Glucose, citric acid and ascorbic acid do not interfere signifi- cantly in the electroanalysis. The proposed electroanalytical procedure can be a promising tool for food safety control.

Keywords

1. Introduction

Carbamates are one of the principal classes of pesticides that are being largely used to increase crop yield. However, their residues may pose serious environmental and health problems [1,2]. The adverse effects of several carbamates were reported, and they include renal, hepatic, neurological, reproductive, immune, and metabolic functions in both humans and animals [3,4]. Some of them are classed as endo- crine disrupting chemicals [5] and regarded as priority pollutants by the United States Environmental Protection Agency [6].

Biosensor technology has been considered as a key tool for the implementation of the new European Union directives because of the negligible waste generation, minimization of use of hazardous substances, high sensitivity and selectivity, as well as, the in situ real- time monitoring capacity [7,8]. In this perspective, the biosensing of environmental pollutants, particularly agrochemicals, using enzymes as biorecognition element has increased pronouncedly in the last years [1,9-14]. Still, many of these devices need to improve their perfor- mance because of the low maximum residue limits (MRLs) established worldwide for pesticides [15,16]. Considerable positive synergistic effects on the current signal can be attained by combining several enzymes [17-21]. Enzyme selection and their sources have a major in- fluence on the biosensor sensitivity [19,22]. The few studies dedicated to bi-enzymatic biosensors [17-21,23-25] reported in the last ten years are summarized in Table 1S (Supplementary material). As far as the authors know, there is no publication related to the application of bi-enzymatic biosensors for the quantification of pesticides in food com- modities or in other real samples. Moreover, there is a general lack of validated biosensor-based procedures for analysis of food samples [1,12,13,26].

The main drawback of the application of enzymatic biosensors to complex matrices is the susceptibility of the transducer to surface passivation. Furthermore, enzymatic products may undergo partial
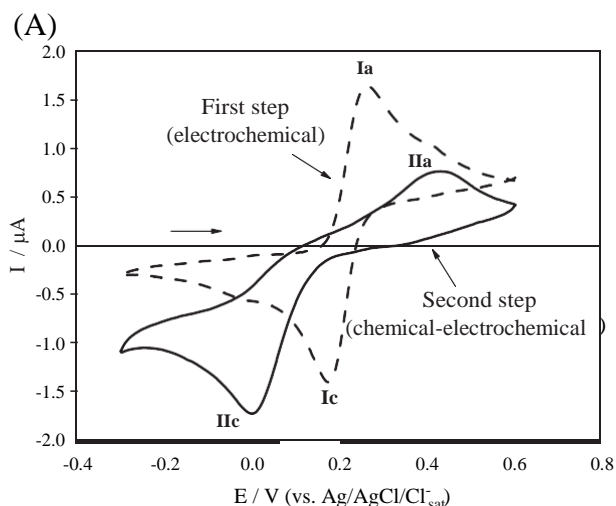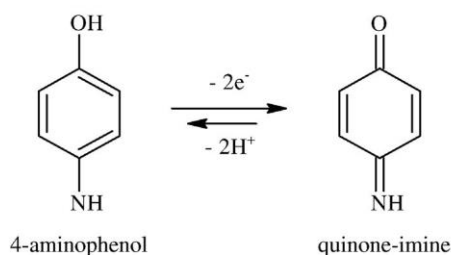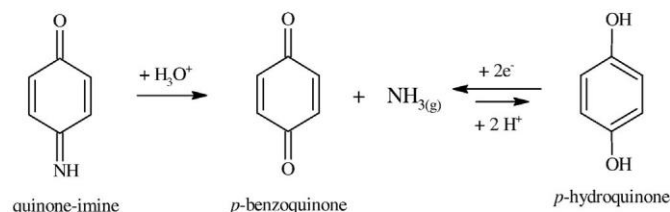
(A)

(B)

(C)

C (87.0%)

O (12.4%)

N (0.60%)

Binding Energy / eV
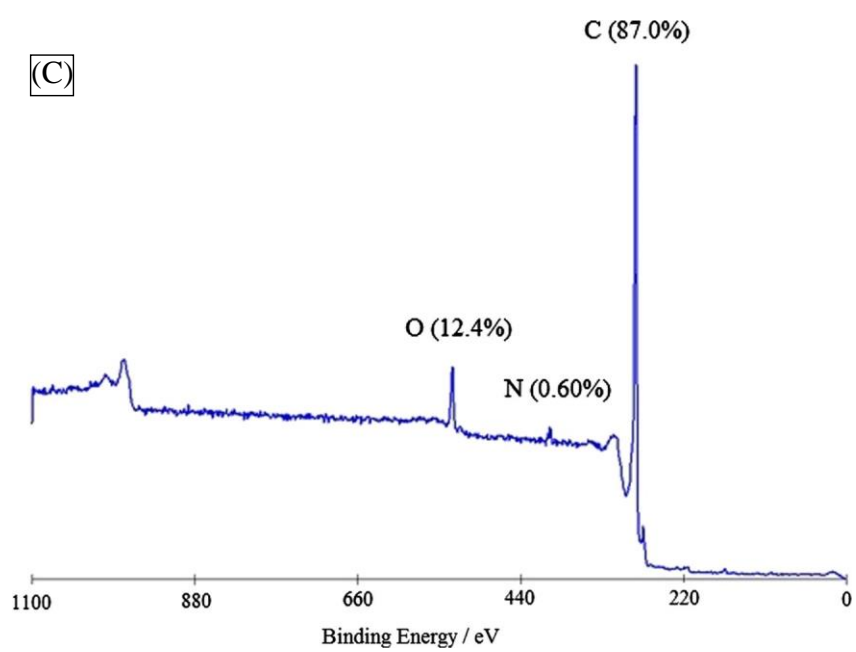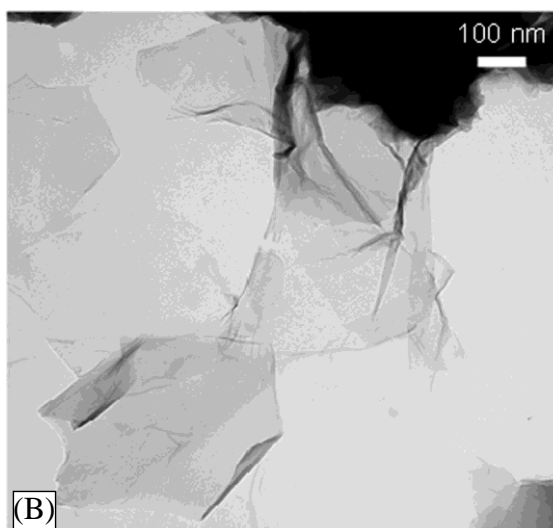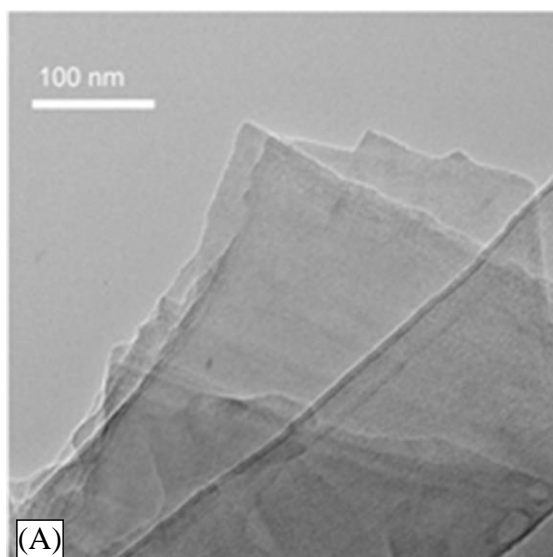
Fig. 2. A) Electrochemical behavior of 4-aminophenol (4.75×10^{-5} M in 0.04 M Britton–Robinson buffer, pH 5.5) obtained with the bare GPE (dashed line) and with the LACC-TYR/GPE (solid line) after an incubation time of 20 min. Scan rate 50 mV/s. B) Mechanistic proposal.
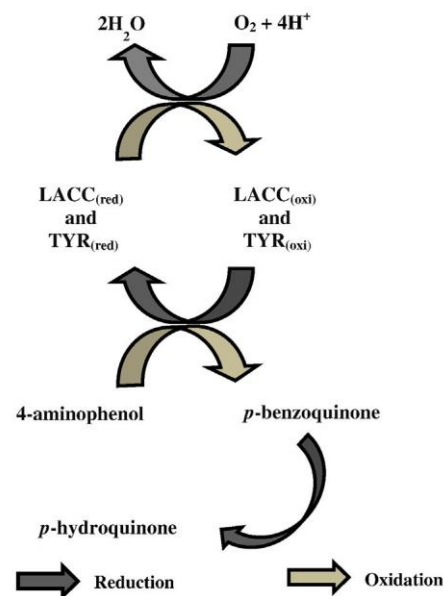
Fig. 2 (*continued*).

electropolymerization onto the bare electrodes, yielding polyaromatic compounds which increase the capacitance and negatively influence the analytical response [19,27]. Protective polymeric films are interesting strategies to overcome these limitations. Chitosan (CS) is a natural polysaccharide which has been extensively studied over the last two decades as a nontoxic, renewable and biodegradable polymer [20,28]. Due to the presence of amino and hydroxyl groups, CS film exhibits multiple functionalities. CS can be cross-linked with nanomaterials [9,20,24,29], inorganic complexes [30], and biological elements [20,31], and used as support for blends with other polymers [32]. CS has excellent membrane-forming ability, high permeability towards water, good adhesion and biocompatibility providing a suitable microenvironment for electroimmobilization of biomolecules on different working surfaces [14,29,33]. However, CS has as main disadvantage to act as an insulator, which hinders the charge-transfer process. In order to improve the current signal, the enrichment of CS matrix with metallic nanoparticles has shown interesting results [21,24,29,33].

Graphene shows great promise for the development of electrochemical biosensors due to its excellent mechanical flexibility, fast electron transfer, and good biocompatibility [13,34–36]. In addition, its electrocatalytic action diminishes the overpotential associated to electroactive compounds, minimizing the interferences that occur in real samples [37]. Graphene can enhance direct electron transfer between enzymes and electrodes. It has been also reported that the use of graphene associated with metal nanoparticles can form exceptionally stable and cost-effective biosensors [35,38]. No graphene-based bi-enzymatic biosensor was found in the literature so far.

Thus, the goal of this study was to explore the synergistic advantages of combining CS (good adhesion and biocompatibility), AuNPs (high superficial area, conductivity and electron transfer rate), two polyphenoloxidases (*Trametes versicolor* laccase, LACC, and *Agaricus bisporus* tyrosinase, TYR, which present high and selective catalytic activity towards phenolic compounds), and a graphene doped carbon paste electrode (20% (w/w); GPE) (high electrocatalytic activity, conductivity and adsorptive character) to prepare a novel bi-enzymatic biosensor. The construction of the device is based on a fast single step electrodeposition of an improved hybrid thin film (LACC-TYR-AuNPs-CS) onto the GPE surface. The developed bi-enzymatic biosensor exhibited high accuracy, precision, sensitivity and stability for quantification of worldwide used carbamates, i.e. formetanate hydrochloride (FMT), carbaryl (CBR), propoxur (PPX) and ziram (ZRM) in citrus (orange, tangerine and lemon) samples.

2. Materials and methods

2.1. Reagents

The polyphenoloxidases LACC (0.5 U mg^{-1}) and TYR (1.0 U mg^{-1}), and the substrate 4-aminophenol (4-AMP) were purchased from

Fig. 1. TEM micrographs of graphene flakes obtained by sonication-assisted exfoliation of graphite in *N*-methyl-2-pyrrolidone before (A) and after (B) the oxidation procedure by Hummers and Offeman method. (C) Representative XPS spectrum of as-prepared graphene flakes obtained by sonication-assisted exfoliation of graphite in *N*-methyl-2-pyrrolidone.

Sigma-Aldrich (Germany). The carbamates CBR (CAS: 63-25-2), FMT (CAS: 23422-53-9), PPX (CAS: 114-26-1) and ZRM (CAS: 137-30-4) were supplied from Fluka (Pestanal®, Germany). Citric and ascorbic acids, and paraffin oil binder were obtained from Merck (Germany). D(+)-glucose anhydrous was from Scharlau (Spain). Spectroscopic grade graphite powder was purchased from Ultracarbon (Spain). Medium molecular weight chitosan (250–300 kDa, DD 93%, apparent viscosity 150 cps) was purchased from Altakitin (Portugal). Other chemicals were of reagent grade and used without further purification. All solutions were prepared with ultrapure water ($\rho = 18 \, M\Omega \, cm^{-1}$) obtained by a Simplicity 185 apparatus (Millipore, Molsheim, France).

Graphene was prepared by sonication-assisted exfoliation of graphite [59]. Briefly, 10 g of graphite powder was sonicated in 100 mL of *N*-methyl-2-pyrrolidone (Sigma-Aldrich) using a probe sonicator with a titanium tip (Bandelin Sonoplus) for 6 h. The dispersion was centrifuged at 500 rpm for 45 min; the supernatant containing the dispersed graphene flakes was removed and then filtered through a nylon 0.2 μm pore size membrane (Whatman). The resulting powder was dried by vacuum, at room temperature, for several days. The Hummers and Offeman method was employed to obtain oxidized graphene. The as-prepared graphene was submitted to a reaction with concentrated sulfuric acid, sodium nitrate, and potassium permanganate in absence of water [39]. Both as-prepared graphene and graphene oxide were characterized by transmission electron microscopy (TEM, Hitachi H-9000NA) with the microscope operating at an accelerating voltage of 200–300 kV. The as-prepared graphene was also characterized by X-ray photoelectron spectroscopy (XPS, VG Scientific ESCALAB 200A spectrometer) using non-monochromatized Al Ka radiation (1486.6 eV).

AuNPs were synthesized by the Turkevich method, through the reduction of 0.01% gold (III) chloride solution by citrate and ascorbic acids [40]. The hydrodynamic size and potential zeta of the nanoparticles were characterized by dynamic light scattering and laser Doppler velocimetry, respectively, using a Zetasizer Nano ZS (Malvern Instruments Ltd., Malvern, UK) at 25 °C.

2.2. Bi-enzymatic biosensor construction

Initially, a carbon paste was prepared by mixing spectroscopic grade graphite powder with a paraffin oil binder (70:30%, w/w) and carefully hand-mixing it in a mortar and pestle. Subsequently, this paste was doped with 20% (w/w) of graphene. This proportion was selected based on prior studies developed by our team [13]. The resultant composite material showed excellent characteristics (high conductivity and electron transfer rate) as transducer. The graphene doped carbon paste was packed into a handmade cavity of a Teflon® tube (1.0 mm internal diameter) and then provided by a stainless steel piston. The GPE surface was smoothed against a plain white paper and rinsed with ultrapure water before each measurement.

The composite material was produced by mixing different amounts of AuNPs, CS solution (1%, w/v), LACC and TYR. CS solution (1%, w/v) was prepared by dissolving 0.1 g chitosan powder in 10 mL of 0.05 M acetic acid solution. Several proportions of AuNPs (10, 20, 30, 40, 50, 60 and 70%, v/v) and CS (1%, w/v) solutions were evaluated. This mixture was then enriched with LACC and TYR in several ratios, namely, 4.0:1.0; 3.0:1.0; 2.0:1.0; 1.0:1.0; 1.0:0.0; 0.0:1.0; 1.0:2.0; 1.0:3.0, and 1.0:4.0% (w/w) to produce the uniform composite material LACC-TYR-AuNPs-CS. The LACC-TYR-AuNPs-CS/GPE biosensor was obtained by immersion of the GPE in the above solution and applying a constant potential of −1.5 V for 200 s [41]. These parameters allow electrodeposition of the hybrid film in a single step. Then, the device was washed with ultrapure water. When not in use, it was stored at 4 °C.

2.3. Electrochemical experiments

Cyclic voltammetry (CV), square-wave voltammetry (SWV) and electrochemical impedance spectroscopy (EIS) assays were performed
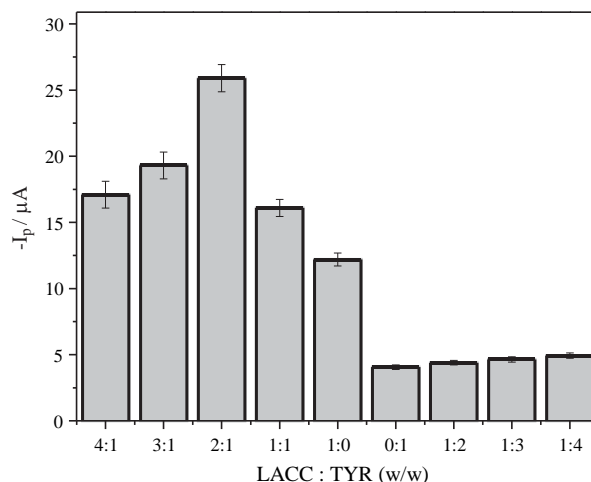

Fig. 3. Intensity of the 4-AMP (4.75×10^{-5} M in Britton–Robinson buffer, pH 5.5) cathodic peak current at −0.07 V obtained with the LACC-TYR-AuNPs-CS/GPE for different ratios (w/w) of LACC and TYR dispersed in the AuNPs-CS composite matrix. Error bars are the standard deviation of three replicates.

at room temperature (20–22 °C) using an electrochemical system Autolab PGSTAT-30 (Eco Chemie, The Netherlands) and GPES/FRA software. The electrochemical cell was assembled with the developed bi-enzymatic biosensor as the working electrode, a Ag/AgCl/KCl (3.0 M) reference electrode, and a platinum counter electrode.

Optimization of the electroanalytical procedure was performed using 4.75×10^{-5} M 4-AMP as substrate in 0.04 M Britton–Robinson buffer (BR; pH 5.5). For the pesticide quantification by the proposed bi-enzymatic biosensor, the SWV parameters, i.e., the frequency, pulse amplitude and height of the potential step were optimized based on the maximum value of peak current (I_p), displacement of the potential peak (E_p), and alterations on half-peak width ($\Delta E_{p/2}$), since their values exert considerable influence on the sensitivity of the electrochemical procedure. The optimal SWV parameters were a frequency of 100 Hz, pulse amplitude of 40 mV and step of 3 mV. The apparent Michaelis–Menten constant K_m (M) was determined using substrate concentrations ranging from 9.90×10^{-6} to 1.23×10^{-4} mol L^{-1} at the optimal experimental parameters.

EIS experiments were performed in the same supporting electrolyte using 4-AMP as redox mediator, for a frequency range from 10^{-1} to 10^5 Hz, amplitude perturbation of 5 mV and applying the half-wave potentials of the 4-AMP reduction peaks in the absence (0.15 V) and in the presence (0.008 V) of the enzymes.

2.4. Electroanalytical characteristics

The selected carbamates were quantified based on their capacity to inhibit the catalytic reaction of the substrate 4.75×10^{-5} M 4-AMP performed by the bi-enzymatic system. The inhibition percentages (IR, %) of the 4-AMP analytical peak at −0.07 V and the concentrations of the different carbamates were employed to obtain the analytical data, according to Eq. (1):

$$\% IR = \left[1 - \left(I_p / I_p^0\right)\right] \times 100 \qquad (1)$$

where I_p^0 and I_p are the peak currents before and after the standard addition of the carbamate pesticides, respectively.

Standard deviations of the intercepts and the average of slopes of the straight lines from the analytical curves were used to determine the detection (LOD) and quantification (LOQ) limits [42].
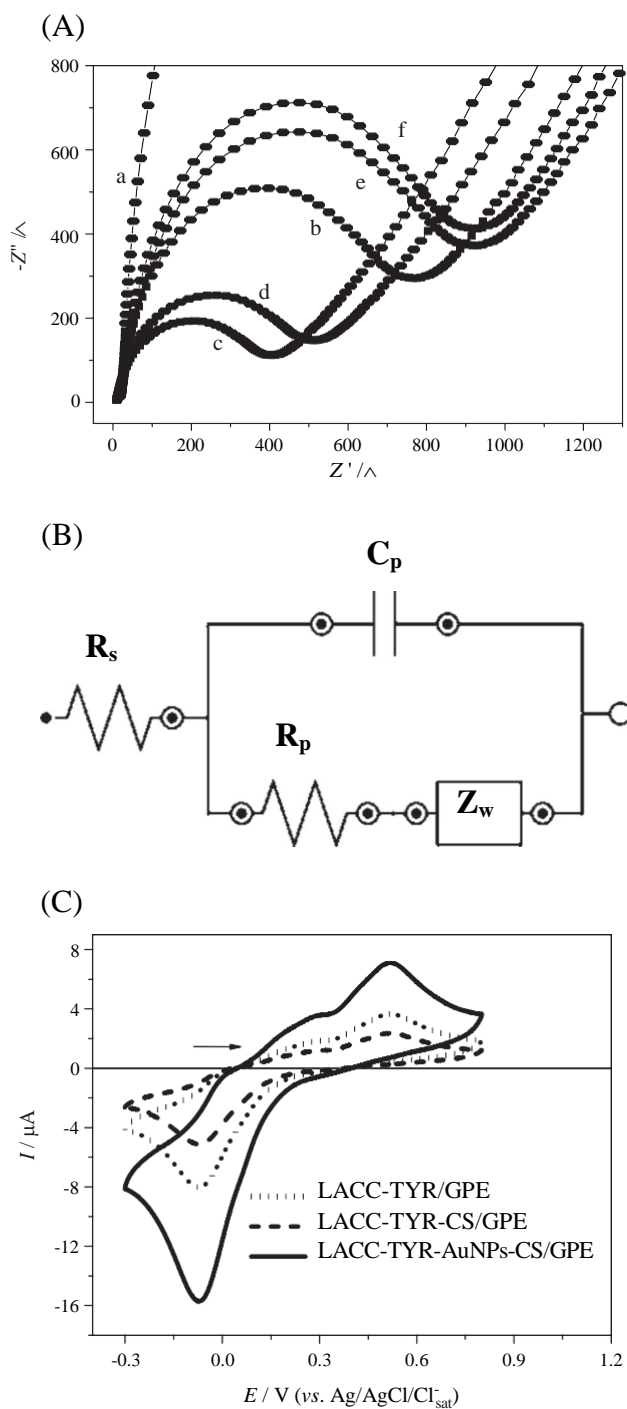
(A)

(B)

(C)

Fig. 4. (A) Nyquist plots of (a) bare GPE, (b) CS/GPE, (c) AuNPs–CS/GPE, (d) LACC-TYR-AuNPs–CS/GPE, (e) LACC-TYR/GPE, and (f) LACC-TYR-CS/GPE, for a frequency range of 10^{-1} to 10^{5} Hz and amplitude perturbation of 5 mV. Experimental conditions: 4.75×10^{-5} M 4-AMP as redox mediator in 0.04 M Britton–Robinson buffer (pH 5.5), conditioning potential of 0.15 and 0.008 V in the absence and in the presence of the enzymes, respectively. (B) Equivalent electrical circuit comprising the resistance of the electrolyte (R_s/Ω), the polarization resistance (R_p/Ω), the Warburg impedance (Z_w/Ω), and the capacitance of the system (C_p/F). (C) Cyclic voltammograms of 4.75×10^{-5} M 4-AMP (Britton–Robinson buffer, pH 5.5) at 50 mV/s on LACC-TYR/GPE, LACC-TYR-CS/GPE, and LACC-TYR-AuNPs–CS/GPE.

2.5. Application to citrus fruits

Samples of orange, tangerine and lemon were obtained from local markets (Oporto region, Portugal), and taken, chopped and homogenized in accordance with guidelines of the European Council Directive [43]. The Quick, Easy, Cheap, Effective, Rugged and Safe – QuEChERS method was
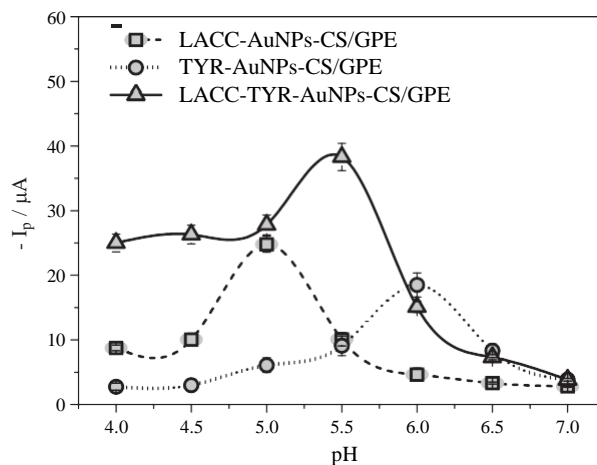

Fig. 5. Relation between I_p and pH obtained with the LACC-AuNPs-CS/GPE (2%), TYR-AuNPs-CS/GPE (1%) and LACC-TYR-AuNPs-CS/GPE (LACC:TYR ratio of 2.0:1.0%, w/w). Experimental conditions: 4.75×10^{-5} M 4-AMP (0.04 M Britton–Robinson buffer), scan rate of 50 mV/s and incubation time of 20 min. Error bars are the standard deviation of three replicates.

employed for the extraction step [44,45]. Briefly, an aliquot of 10 ± 0.05 g of homogenized sample was transferred to a tube containing the buffer-salt mixture 6 g $MgSO_4$/1.5 g NaCl/1.5 g $C_6H_5Na_3O_7 \cdot 2H_2O$ (UCT, Bristol, USA). Next, 10 mL of acetonitrile was added and the QuEChERS tube was shaken vigorously for 1 min. After centrifugation in a 2.16 Sartorius centrifuge (Sigma, Goettingen, Germany), for 3 min at 4000 rpm, the solvent layer was evaporated under vacuum in a Büchi B-940 rotary evaporator (Büchi, Switzerland), and then with a gentle stream of nitrogen to complete dryness. The residue was re-dissolved with 10 mL of 0.04 M BR buffer solution at pH 5.5 containing 4.75×10^{-5} M 4-AMP, immediately before the electroanalysis. Validation of the pesticide residue methodology was performed by recovery assays of fortified citrus samples at two spiking levels (0.01-3.14 mg kg^{-1}). All measurements were carried out in triplicate by the standard addition method.

3. Results and discussion

3.1. Graphene characterization

TEM micrographs of the reduced graphene (Fig. 1A) and oxidized (Fig. 1B) graphene confirm the success of the graphite exfoliation in N-methyl-2-pyrrolidone which produced graphene flakes with few layers, irregular shape and size, different thicknesses, and length varying from ~ 500 nm to ~ 1.5 μm. In addition, it can be observed that the morphology and the size of this nanomaterial were not significantly affected during the oxidation procedure by the Hummers and Offeman method. The influence of the redox state of graphene flakes in the electrochemical signal of the substrate 4-AMP was assessed. The as-prepared reduced graphene showed an analytical signal 2.1 times higher than the oxidized form. This result is due to the higher electric conductivity of the reduced graphene when compared to the oxidized sample, since upon graphene oxidation there is some disruption of the extended π delocalization due to the formation of oxygen group functionalities within graphene layers. Consequently, the reduced form is more adequate for electroanalysis with 4-AMP substrate. XPS surface atomic characterization (Fig. 1C) indicated that the as-prepared reduced graphene is composed by 87.0% carbon, 12.4% oxygen and 0.6% nitrogen. The presence of nitrogen is due to a small contamination of the solvent used (N-methyl-2-pyrrolidone), which doesn't compromise the quality of the material as transducer.

Table 1

Carbamate pesticide calibration and recovery data obtained with the optimized LACC-TYR-AuNPs–CS/GPE biosensor in QuEChERS extracts of citrus fruits. Voltammetric conditions: 4.75×10^{-5} M 4-AMP (0.04 M Britton–Robinson buffer, pH 5.5), frequency 100 Hz, pulse amplitude 40 mV and scan increment 3 mV.

Parameter	[a]CBR	[b]FMT	[c]PPX	[d]ZRM
Linear range/M	9.90×10^{-8} to 2.91×10^{-6}	9.99×10^{-7} to 3.21×10^{-5}	4.99×10^{-7} to 1.92×10^{-5}	9.99×10^{-8} to 3.38×10^{-7}
Intercept/% inhibition	−2.22	6.40	2.99	−2.32
[e]SD$_a$/% inhibition	±0.21	±0.13	±0.08	±0.12
Slope/% inhibition M^{-1}	2.92×10^7	1.82×10^6	1.13×10^6	2.19×10^8
[f]SD$_b$/% inhibition M^{-1}	±1.82×10^6	±1.08×10^5	±8.11×10^4	±2.51×10^7
r	0.9994	0.9992	0.9988	0.9989
[g]LOD/M	1.98×10^{-8}	2.15×10^{-7}	1.87×10^{-7}	1.68×10^{-9}
SD$_{LOD}$/M	±1.22×10^{-10}	±3.41×10^{-9}	±6.03×10^{-9}	±1.18×10^{-10}
[h]LOQ/M	6.60×10^{-8}	7.17×10^{-7}	6.25×10^{-7}	5.62×10^{-9}
SD$_{LOQ}$/M	±4.06×10^{-10}	±8.37×10^{-9}	±9.44×10^{-9}	±3.94×10^{-10}
Spiking assays in citrus fruits				
	[a]CBR	[b]FMT	[c]PPX	[d]ZRM
Spiking level I/(mg/kg)	0.01	0.63	0.52	0.01
Recovery/% in orange	96.3 ± 0.4	95.1 ± 0.1	93.9 ± 0.2	95.6 ± 0.4
Recovery/% in tangerine	95.7 ± 0.2	96.3 ± 0.4	94.2 ± 0.1	96.5 ± 0.1
Recovery/% in lemon	94.9 ± 0.1	94.8 ± 0.6	93.8 ± 0.3	95.2 ± 0.2
Spiking level II/(mg/kg)	0.03	3.14	2.55	0.04
Recovery/% in orange	96.8 ± 0.1	96.1 ± 0.3	95.6 ± 0.2	97.8 ± 0.3
Recovery/% in tangerine	95.7 ± 0.2	96.6 ± 0.3	96.9 ± 0.2	97.3 ± 0.3
Recovery/% in lemon	94.8 ± 0.1	95.4 ± 0.5	96.2 ± 0.1	97.1 ± 0.1

[a] CBR: carbaryl.
[b] FMT: formetanate hydrochloride.
[c] PPX: propoxur.
[d] ZRM: ziram.
[e] SD$_a$: standard deviation of intercept.
[f] SD$_b$: standard deviation of the slope.
[g] LOD: detection limit.
[h] LOQ: quantification limit.

3.2. Bi-enzymatic biosensor construction

3.2.1. Concentration ratio of AuNPs and chitosan in the composite material

CS has a gelification process at pH values below its pKa (~6.5) due to the protonation of the hydroxyl and amine groups. In these conditions, the produced material can be used as microenvironment to electroimmobilize at −1.5 V several materials such as metallic nanoparticles and enzymes onto different surfaces due to its suitable biocompatibility and cross-linking ability [14,25,28,20,41].

In this work, negatively charged AuNPs were used in the CS matrix (pH = 5.5) to enhance the conductivity. The synthesized AuNPs exhibited a mean hydrodynamic diameter of 37 nm and an average zeta potential of −38 mV which indicate a physically stable nanosuspension and low tendency to form aggregates [40]. The effects of the AuNPs in the CS matrix were investigated, after electroimmobilization onto the GPE, through the intensity of the peak current of the substrate 4-AMP (4.75×10^{-5} M in BR buffer at pH 5.5). On a bare GPE, the electrochemical behavior of 4-AMP (evaluated from −0.3 to 0.6 V) is represented by a quasi-reversible process (Fig. 2A) with well-defined anodic (peak I_a at 0.31 V) and cathodic (peak I_c at 0.15 V) peaks, which are related to formation of a quinone-imine derivative (Fig. 2B) [46]. When pure CS was electroimmobilized onto the GPE, a decrease of the peak currents was observed due to the insulating properties of this biopolymer. The proportion of AuNPs in the CS matrix (10, 20, 30, 40, 50, 60 and 70%, v/v) was optimized. A linear increase of the anodic and cathodic (peak I_c at 0.15 V; $-I_p/\mu A = 3.57 \times 10^{-2} \pm 2.31 \times 10^{-4} + 4.99 \times 10^{-2} \pm 1.46 \times 10^{-4}$ [AuNPs:CS]/(% v/v); r = 0.9984; n = 7) peak currents was observed for all ratios tested, suggesting a better conductivity and sensitivity for analytical applications. However, the composite material became less consistent and more susceptible to lixiviation from the GPE surface above 40% (v/v). For this ratio, the values of I_p increased ca. 2.3 times. Based on these results, a proportion of AuNPs 40% (v/v) in the CS solution was selected for the subsequent experiments.

3.2.2. Concentration ratio of LACC and TYR in the hybrid film

In acid conditions, polyphenoloxidases catalyze the oxidation process of 4-AMP (Fig. 2B) [12]. Therefore, the quinone-imine derivative produced in the first step is converted to *p*-benzoquinone at the second step (Fig. 2B), which may be further reduced to *p*-hydroquinone at −0.07 V (peak II_c, Fig. 2A) on the bi-enzymatic biosensor through an irreversible process. This step has a slow kinetic and appears to determine the rate of the redox reaction. In this work, this cathodic peak (peak II_c at −0.07 V) was selected as analytical signal due to its higher intensity and stability.

The optimum proportion of LACC and TYR in the AuNPs–CS composite matrix was determined. According to the optimization results exhibited in Fig. 3, when LACC and TYR are used together, and particularly when LACC exists in larger amounts, there is a clear synergistic effect that promotes the amplification of the 4-AMP electrochemical signal. LACC contributes more significantly than TYR to the catalytic oxidation of the substrate having a higher impact on the increase of the I_p values. The best results were observed for the LACC:TYR ratio of 2.0:1.0% (w/w) (corresponding to 1:1 U/U) which was considered the optimal proportion. These results are similar with those attained by Kochana et al. [19] that co-immobilized the enzymes in a titania gel matrix.

3.3. Electrochemical characterization of the biosensor

Studies were conducted by EIS in order to evaluate the influence of each modification in the interface properties of the biosensor. The obtained Nyquist plots are presented in Fig. 4A, and the equivalent electrical circuit used to fit the electrochemical impedance data is presented in Fig. 4B. According to the standard complex function representation, the impedance data can be described as a real Z'(ω) and an imaginary part Z"(ω) (Eqs. (2)-(3)) [47]:

$$Z'(\omega) = R_s + R_p / \left(1 + \omega^2 \times R_p^2 \times C_p^2\right) \qquad (2)$$
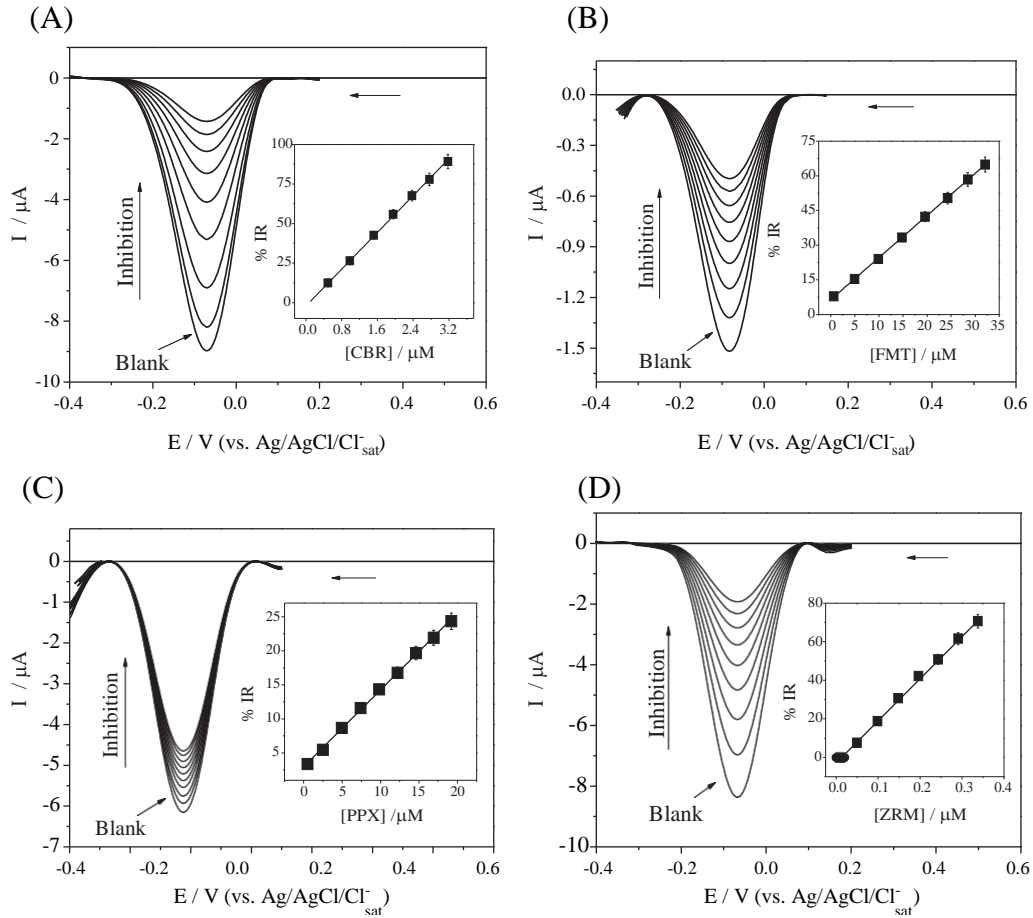
Fig. 6. Square-wave voltammograms of 4.75×10^{-5} M 4-AMP (0.04 M Britton-Robinson buffer, pH 5.5) obtained with the developed LACC-TYR-AuNPs-CS/GPE bi-enzymatic biosensor for quantification of (A) carbaril (CBR; 9.90×10^{-8}-2.91×10^{-6} M), (B) formetanate (FMT; 9.99×10^{-7}-3.21×10^{-5} M), (C) propoxur (PPX; 4.99×10^{-7}-1.92×10^{-5} M) and (D) ziram (ZRM; 9.99×10^{-8}-3.38×10^{-7} M) in QuEChERS extracts of orange samples by the standard addition method. Square-wave voltammetric conditions: frequency 100 Hz, pulse amplitude 40 mV and scan increment 3 mV. The inserts refer to the calibration curves obtained for each carbamate pesticide by inhibition of the enzymatic catalysis (inhibition percentage, %IR $= -2.22 \pm 0.21 + 2.92 \times 10^{7} \pm 1.82 \times 10^{6}$ [CBR]/M; r = 0.9994; n = 8; %IR $= 6.40 \pm 0.13 + 1.82 \times 10^{6} \pm 1.08 \times 10^{5}$ [FMT]/M; r = 0.9992; n = 8; %IR $= 2.99 \pm 0.08 + 1.13 \times 10^{6} \pm 8.11 \times 10^{4}$ [PPX]/M; r = 0.9988; n = 9; %IR $= -2.32 \pm 0.12 + 2.19 \times 10^{8} \pm 2.51 \times 10^{7}$ [ZRM]/M; r = 0.9989; n = 8).

$$-Z''(\omega) = \omega \times R_p^2 \times C_p / \left(1 + \omega^2 \times R_p^2 \times C_p^2\right) \quad (3)$$

where R_s/Ω is the resistance of the electrolyte; R_p/Ω the polarization resistance; C_p/F is the capacitance of the system and ω is the angular frequency ($\omega = 2 \times \pi \times f$; f is the ac-frequency) [47]. GPE showed excellent conductivity and a Z'/−Z'' linear relation (line a), suggesting a mass-transfer process controlled by diffusion. When CS was electrodeposited onto the GPE, a large capacitive arc was observed (line b), indicating an increase of the charge-transfer resistance ($R_{ct} = 767\ \Omega$). However, when CS was enriched with AuNPs (line c), the charge-transfer values decreased sharply ($R_{ct} = 407\ \Omega$), showing that the gold nanoparticles clearly improved the conductivity of the hybrid film.

Regarding the best pathway to immobilize LACC and TYR onto the electrode, cyclic voltammograms of the three alternatives tested, namely, dispersion in the AuNPs-CS composite material, dispersion in pure CS matrix, and directly onto the GPE by drip-coating (solution containing 20 U mL^{-1} LACC and 10 U mL^{-1} TYR) are presented in Fig. 4C while the corresponding EIS results may be observed in Fig. 4A (lines d-f). The lower charge-transfer resistance ($R_{ct} = 527\ \Omega$; Fig. 4A, line d) and consequent higher peak intensity (Fig. 4C) were reached when the enzymes were dispersed in the AuNPs-CS composite. For the other two cases (lines e and f for drip-coating and dispersion in pure CS matrix, respectively), the R_{ct} was higher and quite similar, indicating that the

immobilization processes were also efficient, but in the presence of AuNPs the system exhibited a better performance as electrochemical biosensor. AuNPs are widely used nanomaterials because of their large specific surface area, strong adsorption ability, and high conductivity [33]. Their conductivity characteristics improve the electron transfer between the enzyme redox center and the electrode surface [37]. They can strongly interact with biomaterials and they have been used as a mediator to immobilize biomolecules and to efficiently retain their activity [33].

3.4. Effect of the pH and incubation time on the biosensor response

Although the two selected enzymes are polyphenoloxidases, each one has a different working pH range where maximum activity occurs (2.0-6.0 for LACC and 5.0-8.0 for TYR). Moreover, the optimum pH is highly dependent on the enzyme source and on the substrate used [12,19,22,48]. This experimental parameter is crucial for the development of bi-enzymatic systems. The pH of the electrolyte was ranged from 4 to 7 to characterize the individual activity of LACC and TYR, and the activity of the bi-enzymatic system proposed (Fig. 5). The current response resulting from the enzyme-catalyzed reaction (peak II_c observed at −0.07 V, Fig. 2A) achieved a maximum value at pH 5.0 and 6.0, respectively, for LACC-AuNPs-CS/GPE and TYR-AuNPs-CS/GPE. These results are in accordance to those reported for other individual LACC- and TYR-based biosensors [8,49-51]. By using both enzymes

at the optimum ratio (2.0:1.0, w/w), the peak current was enhanced ca. 1.6 to 2.1 times at pH 5.5 indicating a significant synergistic effect of the LACC-TYR conjugate system. Also, the increase of the pH caused a linear displacement of the peak potential to more negative values $(-E_p/V = -0.64 \pm 0.009 + 0.16 \pm 0.023$ pH; $r = 0.9987$; n = 7) confirming a proton-dependence of the substrate. A pH of 5.5 was selected as the optimum.

The apparent Michaelis-Menten constant K_m (M) [29,52], which reflects both the enzymatic affinity and the kinetic constants was determined based on the Lineweaver-Burk Eq. (4):

$$(1/I_s) = (K_m/I_{max}) \times (1/C) + (1/I_{max}) \qquad (4)$$

where I_s is the steady state current (A) after the addition of substrate, I_{max} corresponds to maximum current (A) obtained in the linear range and C is the concentration (M) of the substrate in the solution. Thus, for a linear regression equation obtained from the relationship between $1/I_s$ and $1/C$ data, the slope and intercept of the linear fit correspond to K_m/I_{max} and $1/I_{max}$, respectively. LACC-TYR-AuNPs-CS/GPE (K_m of 26.9 ± 0.5 M) showed the most interesting properties when compared with the LACC-AuNPs-CS/GPE (K_m of 37.8 ± 0.2 M) and TYR-AuNPs-CS/GPE (K_m of 52.3 ± 0.4 M) since lower K_m values indicate higher grade of affinity of the immobilized enzymes to the substrate [53].

Considering that the analytical peak of the substrate (-0.07 V, peak II_c at Fig. 2A) results from the reduction of the *p*-benzoquinone to *p*-hydroquinone at the second chemical-electrochemical step (Fig. 2B) and that the formation of *p*-benzoquinone is slow and determinant for the reaction rate, the incubation time for the preparation of the biosensor surface was also optimized. The peak current increased until 20 min and remained approximately constant thereafter (data not shown). Thus, this duration was selected as the working incubation/stabilization time before the analytical application of the constructed LACC-TYR-AuNPs-CS/GPE biosensor. Thereafter, and concerning the quantification of the selected carbamates, no incubation time between each SWV measurement was applied.

3.5. Electroanalytical characteristics

Using the optimized square-wave voltammetric parameters (frequency 100 Hz, pulse amplitude 40 mV and scan increment 3 mV), calibration data were obtained for CBR, FMT, PPX and ZRM (Table 1). The lower inhibition percentages were observed for PPX, while the higher were detected for ZRM. These patterns of variation are related with the inherent toxicity of each pesticide for the employed bi-enzymatic system. The analytical curves (Fig. 6) presented wide linear ranges, suitable linearity and low dispersion of the data, even at low concentrations, with correlation coefficients (*r*) ranging from 0.9988 (PPX) to 0.9994 (CBR) (Table 1). The lower LOD and LOQ were reached, by order, for ZRM ᵬ CBR ᵬ PPX ᵬ FMT. The selected carbamates are extensively applied for the protection of fruit and vegetable crops with MRLs ranging from 0.05 to 0.5 mg kg^{-1} (w/w) [16,17]. The attained LODs calculated in a fresh weight basis (0.001 mg kg^{-1} for ZRM, 0.004 mg kg^{-1} for CBR, 0.039 mg kg^{-1} for PPX and 0.048 mg kg^{-1} for FMT) allow application of the electroanalytical procedure for fruit safety quality control.

Repeatability and reproducibility were also assessed by the relative standard deviations (RSD) of different measurements. For intra-day repeatability (n = 10), RSD values ranged from 1.2 to 2.8%, and for inter-day repeatability (n = 5) from 3.2 to 5.8%. Reproducibility studies were made using four different biosensors and the attained RSD varied between 3.2 and 6.5%. The stability of the biosensor was also tested. The catalytic properties of the bi-enzymatic system retained 93.6% of its initial current response over a period of twenty days.

Overall, the results show that the developed LACC-TYR-AuNPs-CS/GPE biosensor presents suitable analytical characteristics for quantification of the selected carbamates. The results achieved with the proposed biosensor are in agreement or compare favorably with those reported previously (scarce and mainly based on acetylcholinesterase) for CBR [54-57], PPX [56], FMT [10,13] and ZRM [13,58].

3.6. Application to citrus fruits

The validation of the biosensor-based procedure was performed by recovery assays performed at two spiking levels (0.01-3.14 mg kg^{-1} w/w) in citrus fruits (orange, tangerine and lemon) (Table 1). Fig. 6 displays representative recovery assays using the standard additions method. Acceptable recoveries for trace pesticides determination were found ranging from 93.9 ± 0.2 to $97.8 \pm 0.3\%$ for orange, from 94.2 ± 0.1 to $97.3 \pm 0.3\%$ for tangerine, and from $93.8 \pm 0.3\%$ to $97.1 \pm 0.1\%$ for lemon samples. The lower recoveries were attained for PPX, while the superior were obtained for ZRM probably due to the different sensitivity of the biosensor to these compounds (the lower for PPX, 1.13×10^{-6} M, and the higher for ZRM, 2.19×10^{-8} M; Table 1). Globally and as expected, a slightly better performance was observed for the higher fortified level tested.

Orange, tangerine and lemon are important sources of glucose, citric acid and ascorbic acid. Consequently, they were tested as possible interferences in the analytical signal of the LACC-TYR-AuNPs-CS/GPE biosensor (results not shown). Experiments were carried out in the presence of several interference:substrate ratios (1:10, 1:1 and 10:1 (v/v)). The higher biases (%) were detected at the maximum ratio which is seldom to occur in 10 g of the analyzed citrus fruits. The results corresponded to a response reduction of $4.7 \pm 0.3\%$ for glucose, ᵬ $7.5 \pm 0.1\%$ for citric acid and ᵬ $11.5 \pm 0.4\%$ for ascorbic acid. Therefore, these results corroborate the reliability of the pesticide residue methodology proposed.

4. Conclusions

In this first study that explores the electrochemical and catalytic properties of a bi-enzymatic device based on a GPE, an accurate and sensitive LACC-TYR-AuNPs-CS/GPE biosensor was developed for carbamate pesticide determination in citrus fruits. The chitosan polymeric matrix produced at pH 5.5 proved to be a suitable microenvironment to carry AuNPs and the selected polyphenoloxidases by a single and fast electrodeposition step onto the GPE. Although pure chitosan increased the charge-transfer resistance of the device, the use of AuNPs allowed overcoming this problem by reducing the R_{ct} of the device, even in the presence of the enzymes. Synergistic positive effects were detected between LACC and TYR at the optimum pH promoting high sensitivity of the proposed bi-enzymatic system. Also, the amine and hydroxyl groups of the chitosan in acid conditions attributed high stability (ca. twenty days) to the biosensor. Thus, the proposed and validated electroanalytical procedures can be an interesting strategy for food safety control of carbamate pesticide residues in fruits. Furthermore, it presents several advantages when compared to the traditional chromatographic techniques employed, namely, it is clearly faster, easier, more environmental friendly while being amenable to integration for in situ determination.

Appendix A. Supplementary data

Supplementary data to this article can be found online at http://dx.doi.org/10.1016/j.bioelechem.2014.02.003.

References

[1] J.S.V. Dyk, B. Pletschke, Review on the use of enzymes for the detection of organo-chlorine, organophosphate and carbamate pesticides in the environment, Chemosphere 82 (2011) 291-307.

[2] S. Morais, E. Dias, M.L. Pereira, Carbamates: human exposure and health effects, in: M. Jokanovic (Ed.), The Impact of Pesticides, WY Academy Press, Cheyenne, 2012, pp. 21-38.

[3] E. Dias, M. Gomes, C. Domingues, E. Ramalheira, S. Morais, M.L. Pereira, Subacute effects of the thiodicarb pesticide on target organs of male Wistar rats: biochemical, histological, and flow cytometry studies, J. Toxicol. Environ. Health A 76 (2013) 533-539.

[4] U. Schulte-Oehlmann, J. Oehlmann, F. Keil, Before the curtain falls: endocrine-active pesticides − a German contamination legacy, Rev. Environ. Contam. Toxicol. 213 (2011) 137-159.

[5] WHO (World Health Organization), State of the Science of Endocrine Disrupting Chemicals 2012, United Nations Environment Programme and the World Health Organization, Geneva, 2013.

[6] US EPA (United States Environmental Protection Agency), National Survey of Pesticides in Drinking Water Wells, Phase II Report, EPA 570/8-91-020, National Technical Information Service, Springfield, 2012.

[7] M. Farré, L. Kantiani, S. Pérez, D. Barceló, Sensors and biosensors in support of EU directives, TrAC, Trends Anal. Chem. 28 (2009) 170-185.

[8] M.D. Fusco, C. Tortolini, D. Deriu, F. Mazzei, Laccase-based biosensor for the determination of polyphenol index in wine, Talanta 81 (2010) 235-240.

[9] C.I.L. Justino, T.A.P. Rocha-Santos, A.C. Duarte, Advances in point-of-care technologies with biosensors based on carbon nanotubes, TrAC, Trends Anal. Chem. 45 (2013) 24-36.

[10] F.W.P. Ribeiro, M.F. Barroso, S. Morais, S. Viswanathan, P. De Lima-Neto, A.N. Correia, M.B.P.P. Oliveira, C. Delerue-Matos, Simple laccase-based biosensor for formetanate hydrochloride quantification in fruits, Bioelectrochemistry 95 (2014) 7-14.

[11] R.K. Shervedani, A. Amini, Direct electrochemistry of dopamine on gold-Agaricus bisporus laccase enzyme electrode: characterization and quantitative detection, Bioelectrochemistry 84 (2012) 25-31.

[12] T.M.B.F. Oliveira, M.F. Barroso, S. Morais, P. De Lima-Neto, A.N. Correia, M.B.P.P. Oliveira, C. Delerue-Matos, Biosensor based on multi-walled carbon nanotubes paste electrode modified with laccase for pirimicarb pesticide quantification, Talanta 106 (2013) 137-143.

[13] T.M.B.F. Oliveira, M.F. Barroso, S. Morais, M. Araújo, C. Freire, P. De Lima-Neto, A.N. Correia, M.B.P.P. Oliveira, C. Delerue-Matos, Laccase-Prussian blue film-graphene doped carbon paste modified electrode for carbamate pesticides quantification, Biosens. Bioelectron. 47 (2013) 292-299.

[14] S. Prakash, T. Chakrabarty, A.K. Singh, V.K. Shahi, Polymer thin films embedded with metal nanoparticles for electrochemical biosensors applications, Biosens. Bioelectron. 41 (2013) 43-53.

[15] EU pesticide residues database, EU pesticide residues database for all the EU-MRLs, (Available at) http://ec.europa.eu/food/plant/protection/pesticides/database (August 2013).

[16] ANVISA (Brazilian Health Surveillance Agency), Monographs of authorized pesticides, (Accessed at) http://portal.anvisa.gov.br/wps/content/Anvisa+Portal/Anvisa/Inicio/Agrotoxicos+e+Toxicologia/Assuntos+de+Interesse/Monografias+de+Agrotoxicos/Monografias (August 2013).

[17] M. ElKaoutit, I. Naranjo-Rodriguez, K.R. Temsamani, M. Domínguez, J.L.H.-H. De Cisneros, Investigation of biosensor signal bioamplification: comparison of direct electrochemistry phenomena of individual laccase, and dual laccase-tyrosinase copper enzymes, at a sonogel-carbon electrode, Talanta 75 (2008) 1348-1355.

[18] O.D. Leite, K.O. Lupetti, O. Fatibello-Filho, I.C. Vieira, A.M. Barbosa, Synergic effect studies of the bi-enzymatic system laccase-peroxidase in a voltammetric biosensor for catecholamines, Talanta 59 (2003) 889-896.

[19] J. Kochana, P. Nowak, A. Jarosz-Wilkołaska, M. Bieroń, Tyrosinase/laccase bienzyme biosensor for amperometric determination of phenolic compounds, Microchem. J. 89 (2008) 171-174.

[20] D. Odaci, A. Telefoncu, S. Timur, Maltose biosensing based on co-immobilization of α-glucosidase and pyranose oxidase, Bioelectrochemistry 79 (2010) 108-113.

[21] E. Zapp, D. Brondani, I.C. Vieira, J. Dupont, C.W. Scheeren, Bioelectroanalytical determination of rutin based on bi-enzymatic sensor containing iridium nanoparticles in ionic liquid phase supported in clay, Electroanalysis 23 (2011) 764-776.

[22] Z. Yang, F. Wu, Catalytic properties of tyrosinase from potato and edible fungi, Biotechnol. 5 (2006) 344-348.

[23] C. Chouteau, S. Dzyadevych, C. Durrieu, J.-M. Chovelon, A bi-enzymatic whole cell conductometric biosensor for heavy metal ions and pesticides detection in water samples, Biosens. Bioelectron. 21 (2005) 273-281.

[24] H. Wang, R. Yuan, Y. Chai, H. Niu, Y. Cao, H. Liu, Bi-enzyme synergetic catalysis to in situ generate coreactant of peroxydisulfate solution for ultrasensitive electrochemiluminescence immunoassay, Biosens. Bioelectron. 37 (2012) 6-10.

[25]

[26] J. Cancino, C.A. Razzino, V. Zucolotto, S.A.S. Machado, The use of mixed self-assembled monolayers as a strategy to improve the efficiency of carbamate detection in environmental monitoring, Electrochim. Acta 87 (2013) 717-723.

[27] M. Diaconu, S.C. Litescu, G.L. Radu, Bienzymatic sensor based on the use of redox enzymes and chitosan-MWCNT nanocomposite. Evaluation of total phenolic content in plant extracts, Microchim. Acta 172 (2011) 177-184.

[28] J. Li, S. Zivanovic, P.M. Davidson, K. Kit, Production and characterization of thick, thin and ultra-thin chitosan/PEO films, Carbohydr. Polym. 83 (2011) 375-382.

[29] C. Zhai, S. Xia, W. Zhao, Z. Gong, X. Wang, Acetylcholinesterase biosensor based on chitosan/Prussian blue/multiwall carbon nanotubes/hollow gold nanospheres nanocomposite film by one-step electrodeposition, Biosens. Bioelectron. 42 (2013) 124-130.

[30] C.L. De Vasconcelos, D.E.S. Dos Santos, T.N.C. Dantas, M.R. Pereira, J.L.C. Fonseca, Effect of molecular weight and ionic strength on the formation of polyelectrolyte complexes based on poly(methacrylic acid) and chitosan, Biomacromolecules 7 (2006) 1245-1252.

[31] S.P. Strand, S. Danielsen, B.E. Christensen, K.M. Vårum, Influence of chitosan structure on the formation and stability of DNA-chitosan polyelectrolyte complexes, Biomacromolecules 6 (2005) 3357-3366.

[32] Y. Martínz, J. Retuert, M. Yazdani-Pedram, H. Cölfen, Hybrid ternary organic-inorganic films based on interpolymer complexes and silica, Polymer 45 (2004) 3257-3265.

[33] K.-J. Huang, J. Li, Y.-Y. Wu, Y.-M. Liu, Amperometric immunobiosensor for α-fetoprotein using Au nanoparticles/chitosan/TiO$_2$-graphene composite based platform, Bioelectrochemistry 90 (2013) 18-23.

[34] M.J. Allen, V.C. Tung, R.B. Kaner, Honeycomb carbon: a review of graphene, Chem. Rev. 110 (2010) 132-145.

[35] T. Kuila, S. Bose, P. Khanra, A.K. Mishra, N.H. Kim, J.H. Lee, Recent advances in graphene-based biosensors, Biosens. Bioelectron. 26 (2011) 4637-4648.

[36] M. Pumera, A. Ambrosi, A. Bonanni, E.L.K. Chng, H.L. Poh, Graphene for electrochemical sensing and biosensing, Trac, Trends Anal. Chem. 29 (2010) 954-965.

[37] A. Sassolas, B. Prieto-Simón, J.-L. Marty, Biosensors for pesticide detection: new trends, Am. J. Anal. Chem. 3 (2012) 210-232.

[38] S. Andreescu, L.A. Luck, Studies of the binding and signaling of surface-immobilized periplasmic glucose receptors on gold nanoparticles: a glucose biosensor application, Anal. Biochem. 375 (2008) 282-290.

[39] C.A. Amarnath, C.E. Hong, N.H. Kim, B.-C. Ku, T. Kuila, J.H. Lee, Efficient synthesis of graphene sheets using pyrrole as a reducing agent, Carbon 49 (2011) 3497-3502.

[40] J. Kimling, M. Maier, B. Okenve, V. Kotaidis, H. Ballot, A. Plech, Turkevich method for gold nanoparticle synthesis revisited, J. Phys. Chem. B 110 (2006) 15700-15707.

[41] M.-H. Xue, Q. Xu, M. Zhou, J.-J. Zhu, In situ immobilization of glucose oxidase in chitosan-gold nanoparticle hybrid film on Prussian blue modified electrode for high-sensitivity glucose detection, Electrochem. Commun. 8 (2006) 1468-1474.

[42] J.N. Miller, J.C. Miller, Statistics and Chemometrics for Analytical Chemistry, Pearson Prentice Hall, United Kingdom, 2005.

[43] European Council Directive 2002/63/CE, Establishing community methods of sampling for the official control of pesticide residues in and on products of plant and animal origin and repealing Directive 79/700/EEC, Off. J. Eur. Communities L187 (2002) 30-31.

[44] M. Anastassiades, S.J. Lehotay, D. Stajnbaher, F.J. Schenck, Fast and easy multiresidue method employing acetonitrile extraction/partitioning and "dispersive solid-phase extraction" for the determination of pesticide residues in produce, J. AOAC Int. 86 (2003) 412-431.

[45] P. Paíga, S. Morais, T. Oliva-Teles, M. Correia, C. Delerue-Matos, S.C. Duarte, A. Pena, C.M. Lino, Extraction of ochratoxin A in bread samples by the QuEChERS methodology, Food Chem. 135 (2012) 2522-2528.

[46] H.J. Salavagione, J. Arias, P. Garcés, E. Morallón, C. Barbero, J.L. Vázquez, Spectroelectrochemical study of the oxidation of aminophenols on platinum electrode in acid medium, J. Electroanal. Chem. 565 (2004) 375-383.

[47] M.E. Orazem, B. Tribollet, Electrochemical Impedance Spectroscopy, John Wiley & Sons, Inc., Hoboken, 2008.

[48] G.-Q. Zhang, G.-J. Chen, H.-X. Wang, T.B. Ng, A laccase with inhibitory activity against HIV-1 reverse transcriptase from the mycorrhizal fungus Lepiota ventriosospora, J. Mol. Catal. B Enzym. 85-86 (2013) 31-36.

[49] E. Casero, M.D. Petit-Domínguez, L. Vázquez, I. Ramírez-Asperilla, A.M. Parra-Alfambra, F. Pariente, E. Lorenzo, Laccase biosensors based on different enzyme immobilization strategies for phenolic compounds determination, Talanta 115 (2013) 401-408.

[50] L. Tang, Y. Zhou, G. Zeng, Z. Li, Y. Liu, Y. Zhang, G. Chen, G. Yang, X. Lei, M. Wu, A tyrosinase biosensor based on ordered mesoporous carbon-Au/L-lysine/Au nanoparticles for simultaneous determination of hydroquinone and catechol, Analyst 138 (2013) 3552-3560.

[51] L. Yang, H. Xiong, X. Zhang, S. Wang, A novel tyrosinase biosensor based on chitosan-carbon-coated nickel nanocomposite film, Bioelectrochemistry 84 (2012) 44-48.

[52] Y. Song, K. Qu, C. Zhao, J. Ren, X. Qu, Graphene oxide: intrinsic peroxidase catalytic activity and its application to glucose detection, Adv. Mater. 22 (2010) 2206-2210.

[53] M. Gamero, F. Pariente, E. Lorenzo, C. Alonso, Nanostructured rough gold electrodes for the development of lactate oxidase-based biosensors, Biosens. Bioelectron. 25 (2010) 2038-2044.

[54] B. Bucur, D. Fournier, A. Danet, J.-L. Marty, Biosensors based on highly sensitive acetylcholinesterases for enhanced carbamate insecticides detection, Anal. Chim. Acta. 562 (2006) 115-121.

[55] J. Caetano, S.A.S. Machado, Determination of carbaryl in tomato "in natura" using an amperometric biosensor based on the inhibition of acetylcholinesterase activity, Sensors Actuators B 129 (2008) 40-46.

[56] G.S. Nunes, D. Barceló, B.S. Grabaric, J.M. Díaz-Cruz, M.L. Ribeiro, Evaluation of a highly sensitive amperometric biosensor with low cholinesterase charge immobilized on a chemically modified carbon paste electrode for trace determination of carbamates in fruit, vegetable and water samples, Anal. Chim. Acta. 399 (1999) 37-49.

[57] X. Wang, L. Chen, S. Xia, Z. Zhu, J. Zhao, J. Chovelon, N.J. Renaul, Tyrosinase biosensor based on interdigitated electrodes for herbicides determination, Int. J. Electrochem. Sci. 1 (2006) 55-61.

[58]

M.T.P. Pita, A.J. Reviejo, F.J.M. Villena, J.M. Pingarrón, Amperometric selective biosensing of dimethyl- and diethyldithiocarbamates based on inhibition processes in a medium of reversed micelles, Anal. Chim. Acta. 340 (1997) 89-97.

[59] U. Khan, I. O'Connor, Y.K. Gun'ko, J.N. Coleman, The Preparation of Hybrid Films of Carbon Nanotubes and Nano-graphite/graphene with Excellent Mechanical and Electrical Properties, Carbon 48 (2010) 2825-2830